C−H···O═C Hydrogen Bonding and Isothermal Crystallization Kinetics of Poly(3-hydroxybutyrate) Investigated by Near-Infrared Spectroscopy

Yun Hu,[†] Jianming Zhang,[†] Harumi Sato,[†] Yoshisuke Futami,[†] Isao Noda,[‡] and Yukihiro Ozaki*,[†]

Department of Chemistry, School of Science and Technology, and Research Center for Environment Friendly Polymers, Kwansei-Gakuin University, Gakuen, Sanda 669-1337, Japan, and The Procter & Gamble Company, 8611 Beckett Road, West Chester, Ohio 45069

Received January 27, 2006; Revised Manuscript Received March 22, 2006

ABSTRACT: We have investigated the C−H···O═C hydrogen bonding and isothermal crystallization kinetics of poly(3-hydroxybutyrate) (PHB) at 125 °C by using near-infrared (NIR) spectroscopy, which allows us to investigate thick films. The NIR spectrum of a PHB film changes remarkably with the evolution of isothermal crystallization process. Accordingly, NIR bands due to the amorphous and crystalline states have been assigned. Particular attention has been paid to a NIR band at 5973 cm^{-1} due to the first overtone of the C−H stretching mode and an IR band at 3435 cm^{-1} due to the first overtone of the C═O stretching mode of the C−H···O═C hydrogen bonding combining two parallel helical structures of PHB. The anharmonicity of C−H (5973 cm^{-1}) and C═O (3435 cm^{-1}) bands arising from the crystalline parts and that of the amorphous C−H (5954 cm^{-1}) and C═O (3457 cm^{-1}) bands was investigated by using both IR and NIR data. The anharmonicity of crystalline C−H and C═O bands is significantly different from that of the amorphous C−H and C═O bands, supporting the idea that both CH and C═O bonds in the crystalline state are involved in the C−H···O═C hydrogen bonding. Principal component analysis (PCA) was used to analyze the real-time NIR difference spectra measured during the isothermal crystallization process. The result suggests that the crystallization process may be not a simple transition of binary mixture of the amorphous and ordered crystalline states. Moreover, the crystallization kinetics parameters of PHB have been obtained by combining PCA and Avrami equation based on the spectral regions instead of the intensity changes of certain bands.

Introduction

Biodegradable polymers have been attracting considerable attention over the recent decades because of their potential contributions to worldwide environmental issues.[1−5] Poly(3-hydroxybutyrate) (PHB) is one of the most extensively studied biodegradable thermoplastic polymers. However, PHB has some disadvantages that limit its use. For example, it is stiff and brittle due to high crystallinity. In addition, its melting temperature is so close to the thermal decomposition temperature that PHB becomes thermally unstable during the processing. Therefore, many attempts have been made to improve the mechanical and thermal properties of PHB, including copolymerization and blending.[6−11] To achieve such a goal, the fundamental understanding of the crystalline structure, physical properties, and crystallization and melting behavior of PHB is essential.

The crystal structure of PHB has been well investigated,[12] which assumes an orthorhombic system $P2_12_12_1$-D^4_2 with a = 5.76 Å, b = 13.20 Å, and c = 5.96 Å (fiber repeat). The recent study by Marchessault et al.[13] suggested that PHB creates the initial self-folding chains from random coil at the first stage of the crystallization, and then the precursor is formed and self-assembled during the PHB lamella crystal formation. Recently, we have investigated the crystallization and melting behavior of PHB and its copolymers, poly(3-hydroxybutyrate-*co*-hydroxyhexanoate) (P(HB-*co*-HHx)), by using wide-angle X-ray diffraction (WAXD),[14,15] infrared (IR) spectroscopy,[16−21] and differential scanning calorimetry (DSC).[14,20] The temperature-dependent WAXD results suggested that there is a particular inter- or intramolecular interaction between the C═O and CH_3 groups, and the interaction becomes weak along the *a* axis of the crystal lattice of PHB with temperature.[14] In IR spectra of PHB, the crystalline CH_3 asymmetric stretching band appears at an anomalously high frequency (3009 cm^{-1}), and the crystalline C═O band at 1723 cm^{-1} shows a downward shift by about 16 cm^{-1} compared with the amorphous C═O stretching band.[16] On the basis of these observations, together with the shorter distance (2.63 Å) between the O atom of the C═O group in one helix structure and the H atom of one of the three C−H bonds of CH_3 group in the other helix structure compared with the sum of the van der Waals separation (2.72 Å), it was concluded that the CH_3 and C═O groups of PHB form a C−H···O═C hydrogen bonding and that a chain of C−H···O═C bonds pair combines the two parallel helical structures.[16] Furthermore, two-dimensional (2D) IR correlation spectroscopy was successfully utilized to characterize the structure variations and conformational changes of PHB during the melt-crystallization process.[21] It was indicated from the 2D IR study that the intensity change in a C═O stretching band at 1731 cm^{-1} is due to an intermediate state and that there is a distinct delay in the intensity change rate between two bands at 1184 and 825 cm^{-1} assignable respectively to the stretching modes of C−O−C and C−C backbones. These results showed that not only the "cooperativity" but also "sequential changes" are responsible for the structural adjustment during the PHB melt-crystallization process.[21]

[†] Kwansei-Gakuin University.
[‡] The Procter & Gamble Company.
* To whom all correspondence should be addressed: Fax +81-79-565-9077; e-mail ozaki@kwansei.ac.jp.

10.1021/ma060208q CCC: $33.50
Published on Web 05/04/2006

IR spectroscopy has played lively roles in the investigations of structural changes during the polymer phase transition because IR bands are very sensitive to the conformation and local molecular environment of polymers.[22−24] However, IR measurements have several requirements in the sample preparation and handling; for example, the thickness of a polymer film must be thin enough. Near-infrared (NIR) spectroscopy, which is concerned with the overtone and combination modes of fundamentals, is also sensitive to structural variations in polymers.[25] In comparison to IR spectroscopy, NIR spectroscopy has certain advantages in studying polymers. In general, sample preparation and handling is much easier for NIR spectroscopy. It can be applied to thick films, sheets, granulates, powders, fibers, and textiles.[25] Furthermore, in conjunction with light-fiber technique, it enables on-line monitoring of polymer reactions and productions.[25−28] In the polymer industry, the direct polymerization analyses and real-time monitoring of physical and chemical properties have long been desired. As optical fiber NIR spectroscopy holds considerable promise for them, many researchers have been investigating on-line polymer process analysis by using it. NIR spectroscopy is also powerful in studying hydrogen bondings, hydration, and inter- and intramolecular interactions in polymers. By combining IR and NIR data, one can explore the anharmonicity of a band which is very sensitive to the formation and strength of a hydrogen bond.[25]

To our knowledge, surprisingly little study has been carried out on the crystallization process of polymers by using NIR spectroscopy. The present study has three purposes. One is to make detailed NIR spectral analysis of PHB and to give the ascription of the amorphous and crystalline bands. Another purpose is to explore the C−H···O═C hydrogen bonding between the CH_3 and C═O groups. For this purpose we calculated the anharmonicity for the C═O and CH bands arriving from both crystalline and amorphous states. Yet another purpose is to investigate the crystallization kinetics of PHB based on NIR spectral variations and principal component analysis (PCA).[29] PCA is a universal and well-established exploratory technique. This technique requires neither any calibration nor any assumption about the kinetics of the process, but it can provide valuable graphical information by analyzing scores and loadings of the principal components, which can be easily used to monitor the crystallization kinetics and spectral variations. This sort of studies provide also solid basis for the real-time NIR monitoring of physical and chemical properties of polymers.

Experimental Section

Materials and Sample Preparation Procedures. Bacterially synthesized PHB with $M_n = 2.9 \times 10^5$ and $M_w = 6.5 \times 10^5$ was obtained from the Procter & Gamble Co., Cincinnati, OH. PHB was purified by first dissolving the sample into hot chloroform and then precipitating in methanol as fine powder and vacuum-drying at 60 °C. For the IR measurement, a PHB film with a thickness of about 10 μm was cast on KBr windows from a 1% (w/v) PHB chloroform solution. After the majority of the solvent had evaporated, the film was placed under vacuum at room temperature for 24 h to completely remove the residual solvent.

A film with 500 μm thickness for the NIR measurement was prepared by compression-molding the PHB powder at 190 °C with a pressure of 25 kg/cm^2 and subsequently quenching quickly into room temperature under vacuum for 24 h.

Measurements. For the IR study of the melt-crystallization process of PHB, the KBr windows with the sample was set on a variable temperature cell (CN4400, OMEGA) with an accuracy of ±0.5 °C, which was placed in the sample compartment of a Thermo Nicolet Magna 870 spectrometer equipped with a MCT detector. IR spectra were measured at a 2 cm^{-1} resolution, and to ensure a high signal-to-noise ratio, 32 scans were coadded.

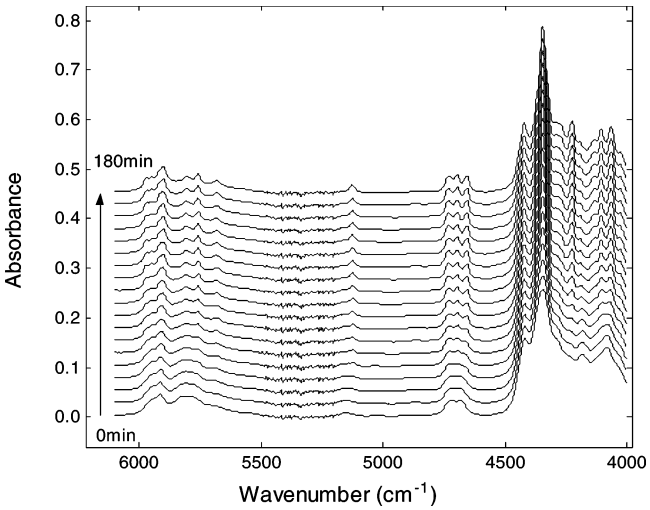

Figure 1. NIR spectra in the region of 6050−4000 cm^{-1} of PHB in a film during the melt-crystallization process at 125 °C. The spectra shown were collected at every 10 min from 0 to 180 min.

A Perkin-Elmer Spectrum One NTS FT-NIR spectrometer equipped with a NIR-TGS detector was used at a 4 cm^{-1} resolution for the NIR measurement. For every spectral measurement, 16 scans were coadded. The temperature of the NIR cell was controlled by the same temperature device as that for the IR measurement.

Both samples were first heated at 10 °C/min up to 195 °C (about 25 °C above the melting point) for 2 min to melt the polymer and erase the thermal history. Then, they were cooled at 5 °C/min to 125 °C for isothermal melt-crystallization. During the cooling period, we monitored spectral changes in PHB with real-time IR and NIR measurements.

Data Analysis. The Unscrambler software program (version 9.2, CAMO AS, Trondhei, Norway) was employed for the data analysis. For the NIR spectra analysis, the spectra in the 6200−4000 cm^{-1} region were subjected to multiplicative scatter correction and a linear baseline correction, followed by offsetting to the zero absorbance value.

Results and Discussion

Time-Dependent NIR Spectra of PHB. Figure 1 displays time-dependent NIR spectra in the range of 6050−4000 cm^{-1} of a PHB film sample during the isothermal melt-crystallization process at 125 °C. It is noted that the NIR spectra are sensitive to the structural changes taking place during the PHB crystallization process.

Figure 2a shows temporal spectral changes in the region of 6050−5650 cm^{-1} of the PHB film aligned at a 20 min interval. Figure 2b depicts the second derivatives of the spectra measured at 0 and 180 min. It can be seen from the second derivative that the spectrum of amorphous PHB is relatively simple in this region and that four amorphous peaks can be detected around 5954, 5913, 5828, and 5768 cm^{-1}. However, the spectrum of the semicrystalline PHB shows at least seven bands at 5973, 5952, 5917, 5900, 5811, 5757, and 5681 cm^{-1} in the same region. Parts a and b of Figure 3 show the corresponding IR spectra in the 3050−2840 cm^{-1} region and the second derivatives of the spectra measured at 0 and 180 min, respectively. Comparison of the temporal NIR spectral variations in the 6050−5650 cm^{-1} region with the corresponding IR spectral changes in the 3050−2840 cm^{-1} region reveals that there are some similarities between them. For example, the NIR band with the highest frequency at 5973 cm^{-1} and the corresponding

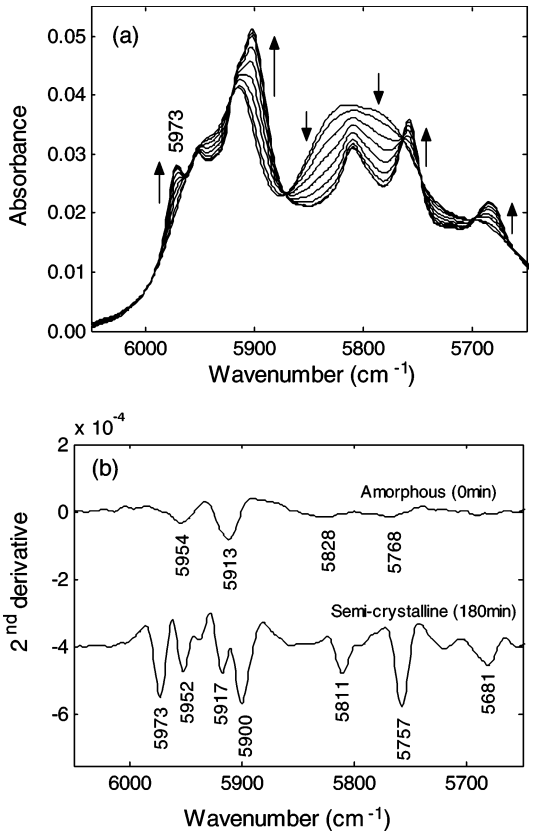

Figure 2. (a) Temporal changes of NIR spectra in the range of 6050−5650 cm^{-1} of the PHB film during the melt-crystallization process at 125 °C. (b) Second derivatives of the spectra measured at 0 and 180 min.

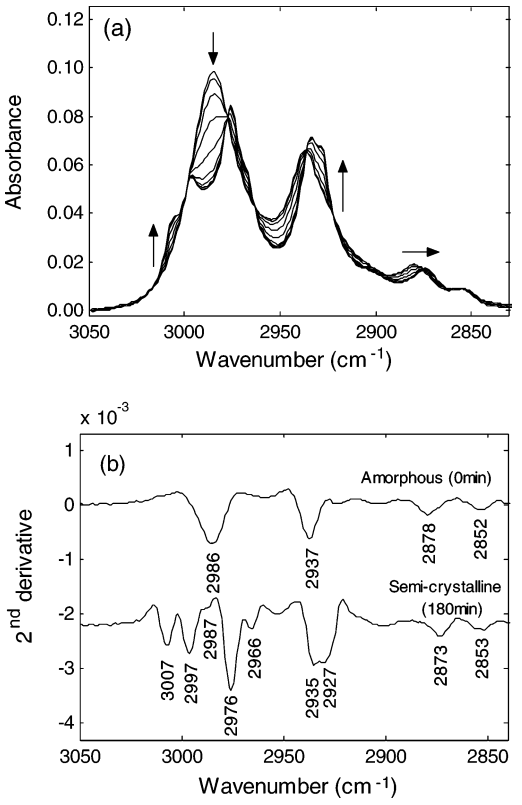

Figure 3. (a) Temporal changes of IR spectra in the range of 3050−2840 cm^{-1} during the melt-crystallization process of the PHB film at 125 °C. (b) Second derivatives of the spectra measured at 0 and 180 min.

IR band at 3007 cm^{-1} show similar trends in temporal changes. Both increase with time, suggesting that they arise from the crystalline state. We analyzed the temporal IR spectral variations in the CH stretching region of PHB during the melt-crystallization process at 129 °C.[21] The results shown in Figure 3 are very close to those reported in our previous study because the difference in the melt-crystallization temperature is small (125 vs 129 °C). According to our previous IR study,[21] bands at 2976 and 2966 cm^{-1} and those at 2935 and 2927 cm^{-1} may be caused by the crystal field splitting. The unusual high wavenumber shift of the CH_3 asymmetric stretching band at 3007 cm^{-1} indicated the existence of a C−H···O═C hydrogen bond.[16,21] Moreover, the CH stretching band shifts from 2878 to 2873 cm^{-1} upon the crystallization (Figure 3b), which reflects the conformational transition from the disordered state to the ordered state.[21] Correspondingly, the NIR bands in the 6050−5650 cm^{-1} region, which arise from the first overtones or combination modes of CH_3, CH_2, and CH stretching vibrations, also change markedly with the development of PHB crystalline structure.

The NIR spectra in the region of 6100−5600 cm^{-1} are heavily overlapped, and thus the band assignments are not straightforward. It is very likely that an amorphous band at 5954 cm^{-1} arises from the first overtone of CH_3 asymmetric stretching mode. It is of note that bands at about 5828 and 5768 cm^{-1} shift to 5811 and 5757 cm^{-1}, respectively, with the evolution of PHB crystallization. Such low-frequency shifts should be related to the disordered to the ordered conformational transition of PHB in the crystallization process.[21] The band at 5973 cm^{-1} in the spectrum of semicrystalline state may be due to the first overtone of the IR band at 3007 cm^{-1} assigned to the CH stretching vibration of the C−H···O═C hydrogen bond. By using the frequencies of a fundamental and its first overtone,

Table 1. Spectroscopic Data for the IR and NIR Region Together with the Calculated Anharmonicity for PHB

band		frequency (cm^{-1}) fundamental	frequency (cm^{-1}) first overtone	X (cm^{-1})
CH	crystalline	3007	5973	−20.5
	amorphous	2986	5954	−9.0
C═O	crystalline	1722	3435	−4.5
	amorphous	1743	3457	−14.5

one can estimate the anharmonicity, which is a very important factor for investigating the nature of hydrogen bonding. In this study, the anharmonicity is estimated by calculating the deviation of the actual fundamental frequency position from the exact half of the fundamental frequency

$$X = \frac{1}{2}\tilde{\nu}_{02} - \tilde{\nu}_{01} \quad (1)$$

Here, $\tilde{\nu}_{0i}$ denotes the wavenumber corresponding to the $i \leftarrow 0$ vibrational transition. Thus, we calculated the anharmonicities of crystalline (5973, 3007 cm^{-1}) and amorphous (5954, 2986 cm^{-1}) C−H bands to be −20.5 and −9.0 cm^{-1}, respectively, from these frequencies according to eq 1. The results for the anharmonicity are listed in Table 1 and will be discussed later together with those of C═O bands.

Figure 4a depicts NIR spectra in the region of 5200−5060 cm^{-1} of PHB during the melt crystallization process. The intensity of a band at 5127 cm^{-1} increases gradually with time, while a broad feature centered at 5160 cm^{-1} decreases during the crystallization process. Thus, it seems reasonable to assign the former band to the crystalline band and the latter band to the amorphous one. Figure 4b displays the corresponding IR spectra in the 1780−1670 cm^{-1} region of PHB, where the bands at 1722 and 1743 cm^{-1} are assigned to the crystalline and

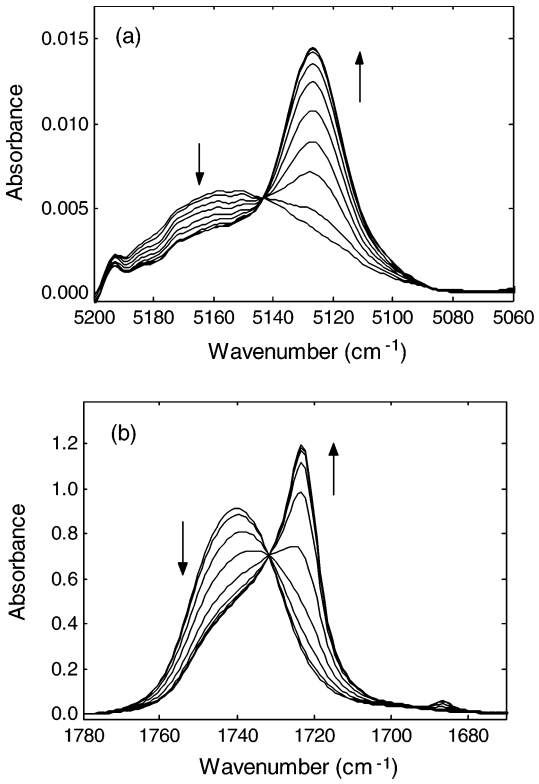

Figure 4. (a) Temporal changes of NIR spectra in the region of 5200−5060 cm^{-1} during the melt-crystallization process of the PHB film at 125 °C. (b) Temporal changes of IR spectra in the region of 1780−1670 cm^{-1} during the melt-crystallization process of the PHB film at 125 °C.

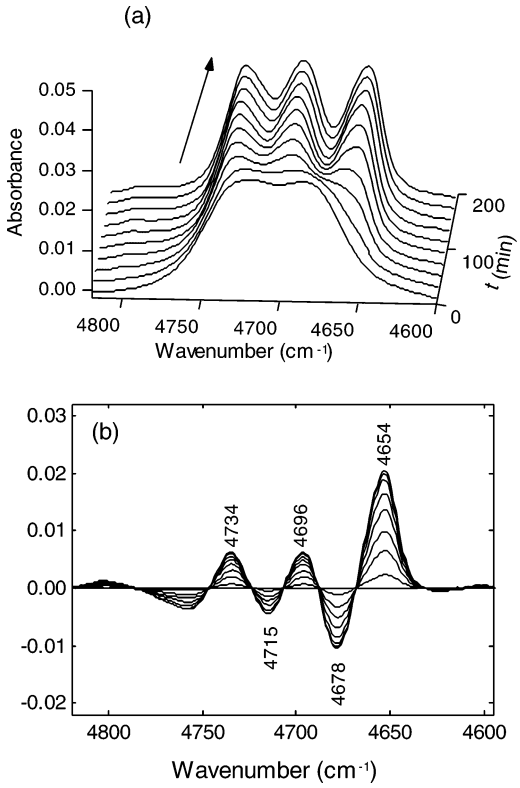

Figure 5. (a) Temporal changes of NIR spectra in the range of 4820−4600 cm^{-1} during the melt-crystallization process of PHB at 125 °C. (b) Difference spectra obtained by the subtraction of the spectrum measured at 0 min from the spectra shown in (a).

amorphous C═O bands, respectively.[16] Comparison of the spectra in Figure 4a with those in Figure 4b suggests that the band at 5127 cm^{-1} is due to the second overtone of the C═O stretching mode of the C−H···O═C hydrogen bonding in the crystalline state, while the broad feature near 5160 cm^{-1} is ascribed to the second overtone of the C═O stretching mode of the amorphous state. The corresponding first overtones are observed at 3435 and 3457 cm^{-1} in the IR spectra. Based on the IR spectral data of the first overtone and fundamental frequencies, the anharmonicity of the crystalline and amorphous C═O bands were calculated respectively to be −4.5 and −14.5 cm^{-1}, as shown in Table 1. It is interestingly noted that the anharmonicity of the crystalline C−H and C═O bands are largely different from that of amorphous C−H and C═O bands. These results for the anharmonicity strongly suggest that the environments surrounding the CH and C═O bonds vary in the amorphous and crystalline states. In the present case, it seems very likely that the large variations in the anharmonicity are caused by the formation of the C−H···O═C hydrogen bonding.

Figure 5a exhibits time-dependent NIR spectral variations in the 4820−4600 cm^{-1} region of PHB during the melt-crystallization process. Figure 5b shows difference spectra calculated by subtracting the initial spectrum (0 min) from the spectra shown in Figure 5a. Upward peaks at 4734, 4696, and 4654 cm^{-1} and downward peaks at 4715 and 4678 cm^{-1} in the difference spectra are respectively assigned to the combination modes of the C═O and CH stretching vibrations of the crystalline and amorphous states. Figure 6a presents the temporal changes of the NIR spectra in the range of 4500−4000 cm^{-1} during the melt-crystallization process of PHB at 125 °C. Seen from the second derivatives of the spectra measured at 0 and 180 min, as exemplified in Figure 6b, the NIR spectra in this region are complicated probably because various combination

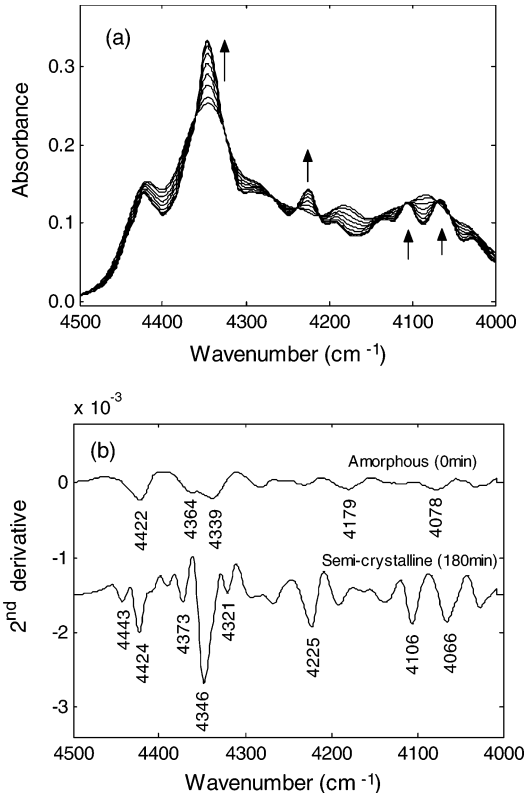

Figure 6. (a) Temporal changes of the NIR spectra in the region of 4500−4000 cm^{-1} during the melt-crystallization process of PHB at 125 °C. (b) Second derivatives of the spectra measured at 0 and 180 min shown in (a).

modes of CH stretching and CH deformation vibrations are expected to appear.

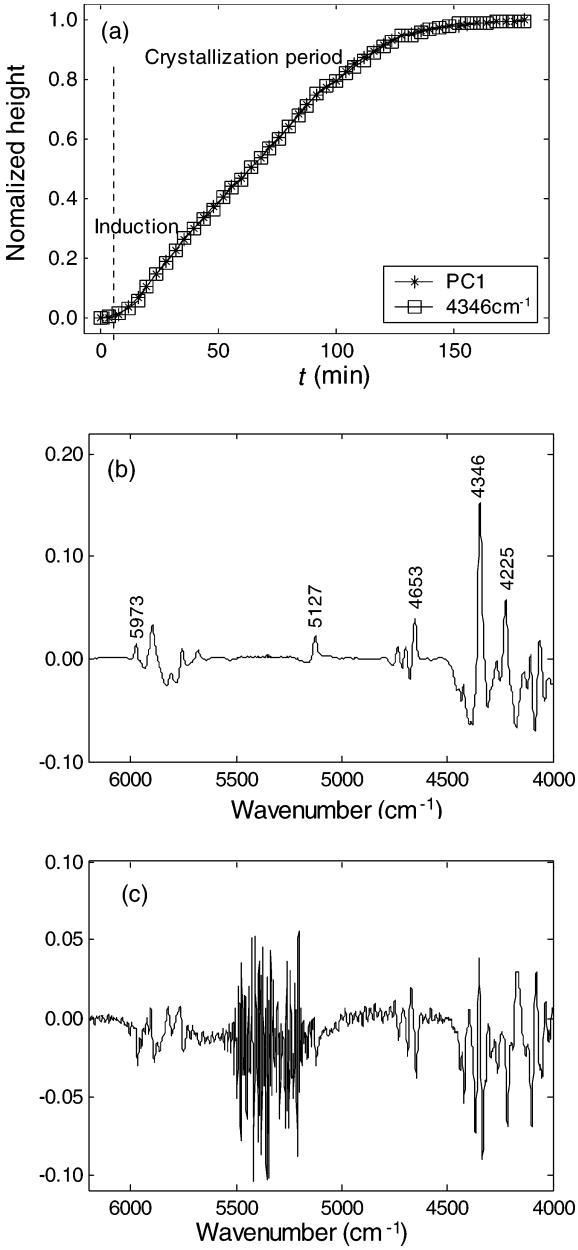

Figure 7. (a) Normalized PC1 score plot (*) and an evolving trace of normalized peak heights of the band at 4346 cm^{-1} (□) with time during the isothermal melt crystallization process of PHB at 125 °C. Loading plots of (b) PC1 and (c) PC2.

Crystallization Kinetics. Usually, the intensity changes of certain vibrational bands can be utilized to monitor the crystallization kinetics of polymers, yet the serious overlapping of spectral peaks makes this analysis difficult. Multivariate analysis techniques are widely used to deal with the large quantities of information extracted from tens or hundreds of measurements. Among them, principal component analysis (PCA)[29] has been the most widely used. PCA helps one explain the pertinent information in a large data set by only using a few factors, so-called principal components (PCs), which provide a reliable access to the variance of the spectral data. Thus, the technique imposes the spectral analysis to become substantially more simplified and pronounced in the pertinent information content. In the present study, PCA was relegated for the crystallization kinetics of PHB.

Figure 7a shows a normalized score plot of the first principal component (PC1) vs the crystallization time, as marked with star sign, obtained from the NIR difference spectra (derived from

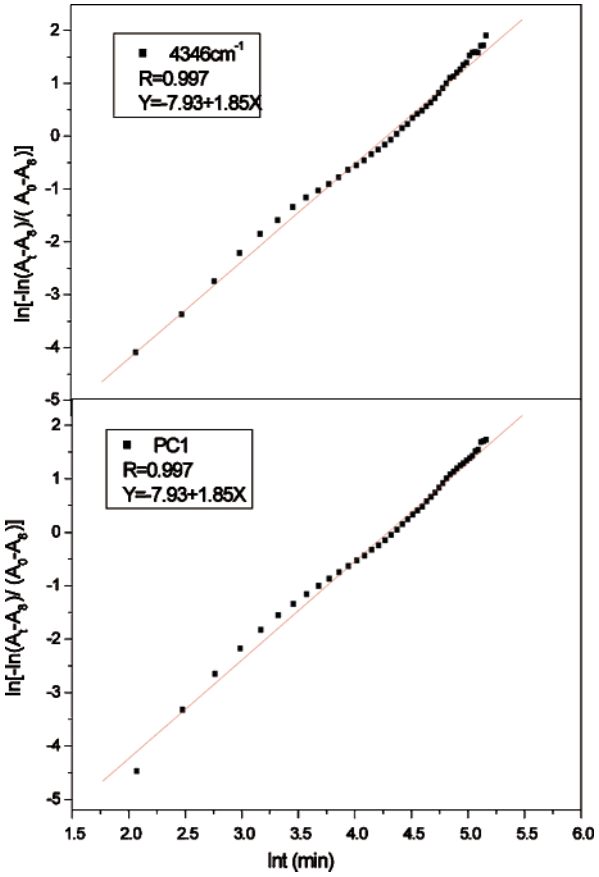

Figure 8. Avrami plot for the isothermal melt crystallization dynamics of PHB at 125 °C derived from the normalized peak height of the band at 4346 cm^{-1} (top panel) and PC1 score of the NIR difference spectra in the 6200−4000 cm^{-1} spectral region (bottom panel).

by the subtraction of the spectrum at 0 min) in the 6200−4000 cm^{-1} region. For comparison, an evolving trace is also made for the band at 4346 cm^{-1} during the crystallization process, whose normalized peak heights in the NIR spectra are represented with the square sign in Figure 7a. Of note, the score plot of PC1 and the evolving trace of the band at 4346 cm^{-1} are coincided with each other, indicating that the score vector of PC1 clearly reflects the crystallization behavior of PHB with time development. The PC1 accounts for 99.932% of the total spectral variance, and its loading plot with respect to the wavenumber is shown in Figure 7b. As can be seen from this figure, the loading of PC1 provides how the spectra change with time, where positive bands as marked are mostly correlated with the crystalline state of PHB. With a variance explanation of 99.932%, it may be considered that PC1 explains about all the spectral changes of importance. However, judging from the shape of the loading (Figure 7c) of the second principal component (PC2), PC2 also gives some spectral information more than noise, although it accounts only for 0.046% of the total variance. There are some possible interpretations for this kind of behavior. One is that during the crystallization process the structural evolution and the development of crystalline structure of PHB may be not a simple transition of the binary mixture system (crystalline and amorphous states). On the basis of our previous two-dimensional IR correlation analysis,[18,21] it was demonstrated that sequential changes of functionalities are also responsible for the structural adjustment of polymer chains except for the cooperative changes during the crystallization process. Meanwhile, spectroscopic evidence of the existent IR band at 1731 cm^{-1} was given to suggest that there might be an intermediate state between the ordered crystalline and disordered

Table 2. Avrami Parameters Calculated from the normalized PC1 Scores of Five Broad Spectral Regions for the Isothermal Crystallization Dynamic Analysis of PHB

	spectral regions used for PCA calculation (cm^{-1})				
parameters	6200−4000	6200−5600	5200−5000	4800−4600	4500−4000
rate constant, k ($min^{-n} \times 10^4$)	3.60	2.70	3.90	2.95	3.56
avrami index, n	1.85	1.93	1.85	1.91	1.85
half-time, $t_{1/2}$ (min)	60	58	57	58	60

amorphous states during the phase transitions. However, more information should be needed for further analysis using other techniques. As for the third and later principal components, both score and loading vectors contain only noise information, which could be expected from the component's low eigenvalues and variance explanatory value. However, the crystallization behavior can be approximated to that of a two-components system without a severe loss of information owing to the large variance explained by PC1. Thus, the score and loading of PC1, which clearly reflect the crystallization kinetics and structural evolution of PHB, can be used to monitor the crystallization process, even though some bands overlap seriously.

As described above, we have analyzed the four individual spectral regions: (A) 6200−5600, (B) 5200−5000, (C) 4800−4600, and (D) 4500−4000 cm^{-1} by performing PCA. They are concerned with respectively the first overtone of CH vibration, the second overtone of C═O vibration, the combination of C−H and C═O vibrations, and the combination of CH vibrations.

It is well-known that the kinetics of isothermal crystallization process of polymer can often be expressed by the Avrami equation[30,31]

$$\frac{A_t - A_\infty}{A_0 - A_\infty} = \exp(-kt^n) \tag{2}$$

where A_t is the peak intensity at the crystallization time t, A_0 and A_∞ are respectively the initial and final intensities of peak during isothermal crystallization, k is the overall kinetic constant of crystallization, t is the time of the crystallization, and n is the Avrami exponent, which is related to the nature of nucleation and to the geometry of the growing crystals. Equation 2 can also be rewritten in the following form:

$$\ln\left[-\ln\left(\frac{A_t - A_\infty}{A_0 - A_\infty}\right)\right] = \ln k + n \ln t \tag{3}$$

Here, the normalized score vector of PC1 in different spectral regions has been used in the Avrami equation. For comparison of the results from PCA with that from the spectral changes of a band, we inset the normalized peak height of a NIR band at 4346 cm^{-1} to eq 3, and plotting the first item vs ln t, two Avrami parameters, n and k, can be obtained from the slope and the intercept, respectively. Figure 8 gives an example of an Avrami plot of the crystallization dynamics of PHB at 125 °C. The curve on the top panel is derived from the normalized peak height of the band at 4346 cm^{-1}. Likewise, another curve is acquired from the normalized PC1 score in the 6200−4000 cm^{-1} region, as shown in the bottom panel of Figure 8. It is found that there is a consistent linear relation between these two Avrami plots in terms of the slopes (Avrami parameter $n = 1.85$) and intercepts (−7.93). They both show an initial linear portion that subsequently tends to level off. This deviation may be due to the secondary crystallization caused by the slower crystallization, crystal perfection, or spherulite impingement in the later stage of the crystallization process.

The half-time for the crystallization, $t_{1/2}$, is an important parameter for the discussion of the crystallization kinetics and can be calculated from n and k, such that

$$t_{1/2} = \left(\frac{\ln 2}{k}\right)^{1/n} \tag{4}$$

The parameters of crystallization kinetics calculated by using the normalized score vector of PC1 of the particular NIR spectra in the five regions together with eqs 3 and 4 are listed in Table 2. Note that the crystallization parameters calculated from the normalized PC1 scores obtained from the individual regions are not completely consistent with each other. Consequently, it is implied that PCA technique can be taken with certain appropriate spectral regions into account to monitor the crystallization process of a polymer and to investigate its local crystallization behavior without considering the prior information. Even if the significant characteristic bands overlap severely and even if the band assignments are sometimes unknown, one can use PCA to explore crystallization kinetics.

For the isothermal melt-crystallization of PHB at 125 °C, the average value of the Avrami exponent is $n \approx 2$, which suggests that during the isothermal process of PHB the crystallization starts from heterogeneous nucleation and that the primary crystallization stage corresponds to a two-dimensional, circular, diffusion-controlled growth of nucleation. In the previous IR study, the Avrami exponent n was calculated to be 2.5 from the IR difference spectra of the crystalline sensitive bands at 1184 and 825 cm^{-1} of PHB during the melt-crystallization process at 129 °C. In addition, the Avrami exponent n obtained from DSC data of PHB at other crystallization temperatures (80−114 °C) was also close to 2.[32,33] It means that the Avrami exponent n from the first score vector of NIR data is consistent with those from IR and DSC data. On the basis of the above analysis, the crystallization kinetics can be simply obtained by monitoring score and loading plots of the principal components.

Conclusion

The C−H···O═C hydrogen bonding and crystallization dynamics of PHB have been investigated by using NIR spectroscopy. The spectral changes upon the crystallization process and their band assignments have been analyzed in detail in each spectral region. By comparing the NIR spectra with the corresponding IR spectra, the anharmonicity of the crystalline CH and C═O bands and those of amorphous CH and C═O bands have been calculated. The large changes in the anharmonicity support the idea that the CH and C═O groups form the C−H···O═C hydrogen bonding in the crystalline state. Furthermore, the crystallization kinetics has been explored by combining PCA with the Avrami equation. It has been found that score and corresponding loading plots derived from PCA can analyze the whole crystallization process of polymers instead of using the intensity change of some certain peaks, especially when these peaks are seriously overlapped. This study has provided the fundamental information for NIR spectra to be used in the on-line monitoring of the chemical and physical properties of PHB.

Acknowledgment. We thank Dr. He Huang of Kwansei-Gakuin University, Japan, for valuable discussions. This work was partially supported by "Open Research Center" project for private universities: matching fund subsidy from MEXT (Ministry of Education, Culture, Sports, Science and Technology), 2001−2005. This work was also supported by Kwansei-Gakuin University "Special Research" project, 2004−2008.

References and Notes

(1) Doi, Y. *Microbial Polyesters*; VCH Publishers: New York, 1990.
(2) Kobayashi, G.; Shiotani, T.; Shima, Y.; Doi, Y. In *Biodegradable Plastics and Polymers*; Doi, Y., Fukuda, K., Eds.; Elsevier: Amsterdam, 1994.
(3) Vert, M. *Biomacromolecule*s **2005**, *6*, 538.
(4) Bastioli, C. *Handbook of Biodegradable Polymers*; Rapra Technology Limited: UK, 2005.
(5) Chiellini, E.; Solaro, R. *Recent Advances in Biodegradable Polymers and Plastics*; Wiley-VCH: Weinheim, 2003.
(6) Kunioka, M.; Tamaki, A.; Doi, Y. *Macromolecules* **1989**, *22*, 694.
(7) Doi, Y.; Kitamura, S.; Abe, H. *Macromolecules* **1995**, *28*, 4822.
(8) Ishida, K.; Asakawa, N.; Inoue, Y. *Macromol. Symp.* **2005**, *224*, 47.
(9) Mohamed, K. H.; Samir, A. A.; Omar, M. E.; Mohamed, A. S.; Noda, I.; James, E. M. *J. Appl. Polym. Sci.* **2004**, *94*, 2257.
(10) Chan, C. H.; Kummerlöwe, C.; Kammer, H. W. *Macromol. Chem. Phys.* **2004**, *205*, 664.
(11) Chun, Y. S.; Kim, W. N. *Polymer* **2000**, *41*, 2305.
(12) Yokouchi, M.; Chatani, Y.; Tadokoro, H.; Teranishi, K.; Tani, H. *Polymer* **1973**, *14*, 267.
(13) Marchessault, R. H.; Kawada, J. *Macromolecules* **2004**, *37*, 7418.
(14) Sato, H.; Nakamura, M.; Padermshoke, A.; Yamaguchi, H.; Terauchi, H.; Ekgasit, S.; Noda, I.; Ozaki, Y. *Macromolecules* **2004**, *37*, 3763.
(15) Sato, H.; Mori, K.; Rumi, M.; Ando, Y.; Tagahashi, I.; Zhang, J. M.; Terauchi, H.; Hirose, F.; Senda, K.; Tashiro, K.; Noda, I.; Ozaki, Y. *Macromolecules* **2006**, *39*, 1525.
(16) Sato, H.; Murakami, R.; Padermshoke, A.; Hirose, F.; Senda, K.; Noda, I.; Ozaki, Y. *Macromolecules* **2004**, *37*, 7203.
(17) Sato, H.; Dybal, J.; Murakami, R.; Noda, I.; Ozaki, Y. *J. Mol. Struct.* **2005**, *744*−*747*, 35.
(18) Padermshoke, A.; Katsumoto, Y.; Sato, H.; Ekgasit, S.; Noda, I.; Ozaki, Y. *Spectrochim. Acta, Part A* **2005**, *61*, 541.
(19) Padermshoke, A.; Katsumoto, Y.; Sato, H.; Ekgasit, S.; Noda, I.; Ozaki, Y. *Polymer* **2004**, *45*, 6547.
(20) Sato, H.; Padermshoke, A.; Nakamura, M.; Murakami, R.; Hirose, F.; Senda, K.; Terauchi, H.; Ekgasit, S.; Noda, I.; Ozaki, Y. *Macromol. Symp.* **2005**, *220*, 123.
(21) Zhang, J. M.; Sato, H.; Noda, I.; Ozaki, Y. *Macromolecules* **2005**, *38*, 4274.
(22) Christy, A. A.; Ozaki, Y.; Gregoriou, V. G. *Modern Fourier: Transform Infrared Spectroscopy*; Elsevier: Amsterdam, The Netherlands, 2001.
(23) Kuptsov, A. H.; Zhizhin, G. N. *Handbook of Fourier Transform Raman and Infrared Spectra of Polymers*; Elsevier: Oxford, UK, 1998.
(24) Koenig, J. L. *Spectroscopy of Polymers*; American Chemical Society: Washington, DC, 1992.
(25) Siesler, H. W., Ozaki, Y., Kawata, S., Heise, H. M., Eds. *Near-infrared Spectroscopy*; Wiley-VCH: New York, 2002.
(26) Khettry, A.; Hansen, M. G. *Polym. Eng. Sci.* **1996**, *36*, 1232.
(27) Rohe, T.; Becker, W.; Krey, A.; Nägele, H.; Kölle, S.; Eisenreich, N. *J. Near Infrared Spectrosc.* **1998**, *6*, 325.
(28) Watari, M.; Hisamitsu, H.; Naoto, M.; Masahiro, T.; Ozaki, Y. *Appl. Spectrosc.* **2004**, *58*, 248.
(29) Wold, S.; Esbensen, K.; Geladi, P. *Chemom. Intell. Lab. Syst.* **1987**, *2*, 37.
(30) Avrami, M. *J. Chem. Phys.* **1939**, *7*, 1103.
(31) Avrami, M. *J. Chem. Phys.* **1940**, *8*, 212.
(32) Gunaratne, L. M. W. K.; Hanks, R. A. S. *Eur. Polym. J.* **2005**, *41*, 2980.
(33) Kai, W. K.; He, Y.; Inoue, Y. *Polym. Int.* **2005**, *54*, 780.

MA060208Q